Electronic Research Archive

https://www.aimspress.com/journal/era

ERA, 34(8): 5478–5495.
DOI: 10.3934/era.2026245
Received: 03 March 2026
Revised: 29 May 2026
Accepted: 08 June 2026
Published: 30 June 2026

Research article

Hopf bifurcation analysis in delayed predator-prey models with the Crowley-Martin functional response

Shuang Guo*, **Xing Qiao and Dan Ma**

School of Mathematical Sciences, Daqing Normal University, Daqing 163712, China

* **Correspondence:** Email: guofeixue721030@163.com.

Abstract: A class of delayed predator-prey models with the Crowley-Martin functional response was investigated in this study. First, the conditions for the stability of the coexistence equilibrium were obtained. Second, by applying the normal form method and the center manifold theorem, the conditions for the occurrence of a Hopf bifurcation induced by the time delay were established, and the direction of the Hopf bifurcation was determined. Finally, numerical simulations were conducted to illustrate the theoretical results. The findings provided insights into the effects of time delay on stability and oscillatory behavior in predator-prey interactions, which are significant for understanding population dynamics in ecology.

Keywords: predator-prey model; delay; Hopf bifurcation; Crowley-Martin functional response

1. Introduction

Population ecological models are typically employed to depict the quantitative relationships between population dynamics and key parameters, including birth, death, immigration, and emigration. Population models constitute a key research focus in ecology [1–3]. The predator-prey framework represents one of the most fundamental frameworks in ecology and mathematical biology. It is generally believed that the earliest predator-prey model was proposed by the American population ecologist Alfred Lotka and the Italian mathematician Vito Volterra, and this model is widely recognized as the Lotka-Volterra model:

$$\begin{cases} \dfrac{du(t)}{dt} = a_1 u - b_1 uv, \\ \dfrac{dv(t)}{dt} = -a_2 v - b_2 uv, \end{cases} \tag{1.1}$$

where u and v represent the densities of the population of prey and predators, respectively. a_1, b_1, a_2, b_2 are prey's birth rate, predator's capture rate, the predator's death rate and prey conversion

rate, respectively. However, further research has revealed that predator-prey dynamics in natural ecosystems are far more complex than that depicted by the Lotka-Volterra model. Factors such as predator behavior, prey defense mechanisms, environmental heterogeneity, as well as intraspecific competition and interspecific competition, need to be taken into account [4–6]. The dynamic behavior of a system is strongly dependent on the functional response. The functional response describes the relationship between the quantity of prey consumption unit time and prey density. It not only reflects the predator's predation capacity but also determines the conversion of biological populations and the system's overall dynamic characteristics. Therefore, a more general two-species predator-prey model than the Lotka-Volterra model is given by:

$$\begin{cases} \dfrac{du(t)}{dt} = ug(u) - \phi(u)v, \\ \dfrac{dv(t)}{dt} = kh(u)v - p(v)v, \end{cases} \tag{1.2}$$

where $g(u), h(u)$ are the intrinsic growth rate of prey and predator, respectively, and $\phi(u)$ are predator's functional response function.

Generally, there are four different types of functional response: Holling type I, II, III, and IV. Nonetheless, these four types of functional response functions only depend on the prey population density and have nothing to do with the predator's population density [7, 8]. For example, Holling type II functional response function

$$p(u) = \frac{bu}{1 + au}, a, b > 0$$

describes the average feeding rate of a predator when the predator spends some time searching for prey and some time processing the captured prey , where a and b describe the handling time and the capture rate.

This type of functional response generally occurs when the predation is not interfered by others' actions [9], so these assumptions are sometimes unrealistic. In some cases, the density of predators increases, leading to intensified interference among them, thereby resulting in a decrease in the predation rate. Consequently, predator interference exerts a highly significant effect on the predation rate. Thus, in order to characterize the aforementioned interference among predators, the function is given as

$$p(u, v) = \frac{bu}{1 + au + cv}, (a, b, c > 0),$$

which is called the Beddington-DeAngelis functional response, where c represents the extent of predators' interference with one another.

In 1989, Crowley and Martin revised the above assumptions, positing that predators would interfere with one another while searching for or hunting prey. Based on this assumption, the following function was considered [10]:

$$\phi(u, v) = \frac{mu}{(1 + au)(1 + bv)},$$

where m represents the capture rate; a denotes the effect of time needed by predator to process a unit quantity of prey; and b characterizes the mutual interference between predators. The Crowley-Martin functional response demonstrates broad applicability and enhances explanatory power. When certain parameters take specific values, the models can be reduced to the Holling type I or Holling type II,

thereby demonstrating its close connection with classical models. The Crowley-Martin functional response has been well-researched, demonstrating a consistency between theoretical and empirical values [11–13]. For instance, the Crowley-Martin type functional response in [11] is adopted to analyze the global stability under abundant prey and predator populations. Moreover, by taking the time delay as bifurcation parameter, this study explores the dynamic behavior of the system. It also analyzes the stability of the resulting periodic solutions and determined the direction of the Hopf bifurcation. In [12], the authors studied an advanced Leslie-Gower predator-prey model with the Crowley-Martin-type functional response. They analyzed the local stability of the equilibrium points within the ordinary differential equation framework using bifurcation theory. In order to study a predator-prey system with impulsive effects and the Crowley-Martin functional response, the authors of [13] first constructed an equivalent system without impulses. They analyzed existence and uniqueness of a global solution for the model. Lastly, they applied coincidence degree theory to demonstrate that the system with the Crowley-Martin functional response has positive periodic solutions. [14] described a predator-prey framework that incorporated the Crowley-Martin functional response and the Allee effect. These response functions were used to modify both the predator's self-limitation term and the Allee effect. The authors identified several bifurcations such as Hopf and transcritical bifurcation. In [15], the authors employed characteristic equations and the Routh-Hurwitz criterion, and examined the stability of a Gause-type predator-prey model with the Crowley-Martin functional response. They analyzed the existence of Hopf bifurcation and other dynamical properties. Wang et al. [16] investigated a diffusive predator-prey model with the Crowley-Martin functional response. They found that repulsive prey-taxis can drive spatial pattern formation via non-Turing mechanisms, including spots, stripes, labyrinths, spiral waves, and chaos.

The aforementioned studies mainly investigated Turing patterns, stability behaviors, and Hopf bifurcation in delay-free predator-prey systems, as well as prey-taxis-induced spatial patterns independent of the Crowley-Martin functional responses and time delays. Therefore, there remains a research gap concerning the complex dynamical behaviors, such as period-doubling bifurcation and double Hopf bifurcation in delayed Crowley-Martin predator-prey models. This study fills this research gap by exploring delay-triggered Hopf bifurcation, stability switches, and chaotic dynamical evolution of the model.

Time delays play a substantial and non-negligible role in dynamical systems. The incorporation of time delay terms enables more accurate analysis of the dynamical behaviors of complex systems. In population dynamics models, time delays generally characterize the dependence of population variations on historical states. For predator-prey models, the introduction of time delays may induce periodic oscillations that replace stable steady states or existing chaotic dynamics, which may further result in heterogeneous population distributions and even local population extinction. A large number of studies have adopted functional differential equation theory to explore diverse dynamical phenomena in ecological models [17, 18]. From a biological perspective, time delays reflect the response speed of ecosystems to environmental perturbations and the adaptability of biological populations to variable environments. The existence of time delays enhances the sensitivity of ecosystems to external changes while providing sufficient time for population adjustment and adaptation.

The remainder of this paper is organized as follows. Section 2 presents the model formulation. In Section 3, the Hopf bifurcation and local stability of coexisting equilibrium are investigated via

characteristic equation analysis. In Section 4, the center manifold theorem and normal form method are applied to derive explicit analytical formulas, which determine the stability and bifurcation direction of periodic solutions originating from Hopf bifurcation. Section 5 conducts numerical simulations to verify the theoretical analytical results and predict the evolutionary trends of population densities. Finally, Section 6 concludes the entire work and summarizes the core findings.

2. The mathematical model

In this work we consider the following predator-prey model with Crowley-Martin functional response:

$$\begin{cases} \dfrac{du(t)}{dt} = ru\left(1 - \dfrac{u}{K}\right) - \dfrac{muv}{(1+au)(1+bv)}, \\ \dfrac{dv(t)}{dt} = cv\left(1 - \dfrac{v}{hu}\right), \end{cases} \tag{2.1}$$

where r, K, c, and h denote positive parameters that represent the inherent growth rate of prey, carrying capacity, conversion rate, and predator death rate.

We directly incorporate the time delay into the functional response to represent that the rate at which predators actually consume prey depends on the prey density encountered in the past. The time delay τ introduced into the functional response is intended to capture "the effect of the predator's digestion and assimilation time on the current predation rate". This delay indirectly influences the prey equation because the predator's current predation intensity is modulated by its past food intake (i.e., its satiation level affects its searching and attacking behavior). Moreover, after experiencing predation risk, prey may alter their spatial use or exhibit vigilance behavior for a period of time, causing the current risk of being preyed upon to be correlated with past predation pressure. In this context, the time delay in the functional response can be interpreted as a "fear delay" or "risk memory" . This time delay can also be interpreted as the time lag exhibited by prey after perceiving changes in environmental pressure-such as taking cover, seeking refuge, or altering group behavior. The establishment of such defense mechanisms is not instantaneous. A delay term is introduced into model (2.1) under the assumption that the predators spend a certain amount of time capturing prey:

$$\begin{cases} \dfrac{du(t)}{dt} = ru(1 - \dfrac{u}{K}) - \dfrac{mu(t-\tau)v}{(1+au)(1+bv)}, \\ \dfrac{dv(t)}{dt} = cv(1 - \dfrac{v}{hu}). \end{cases} \tag{2.2}$$

For analytical convenience, we nondimensionalize the model (2.2)

$$rt \to t, \frac{u}{K} \to u, \frac{mKh}{r} \to m, aK \to a, bKh \to b, \frac{c}{r} \to c.$$

Then, model (2.2) is simplified to:

$$\begin{cases} \dfrac{du(t)}{dt} = u(1-u) - \dfrac{mu(t-\tau)v}{(1+au)(1+bv)}, \\ \dfrac{dv(t)}{dt} = cv(1 - \dfrac{v}{u}). \end{cases} \tag{2.3}$$

The introduction of a time delay makes the analysis of characteristic root distribution at the fixed point of the dynamical system highly complicated. This analysis, however, is essential for detecting Hopf bifurcations. In 2001, Ruan and Wei [19] established sufficient conditions under which the total number (counting multiplicities) of zeros of exponential polynomials lie in the right-half complex plane, which provided a theoretical foundation for examining root distributions of a class of delay differential equations. Next, we derive the conditions for Hopf bifurcation in model (2.3).

3. Stability analysis and Hopf bifurcation of coexisting equilibrium

Time delay has no effect on the number of equilibrium points, and nondimensionalization does not alter the essential characteristics of the system. Analysis reveals that model (2.3) has three equilibrium points: $E_1(0,0)$, $E_2(1,0)$, $\overline{E}\ (u^*, v^*)$, while u^*, v^* satisfy the following two equations:

$$1 - u^* - \frac{mv^*}{(1+au^*)(1+bv^*)} = 0, \quad \frac{v^*}{u^*} = 1,$$

from which we furthur derive their values as followed:

$$u^* = v^* = \sqrt[3]{m_{13} + \sqrt{m_{13}^2 + (m_{11} - m_{12}^2)^3}} + \sqrt[3]{m_{13} - \sqrt{m_{13}^2 + (m_{11} - m_{12}^2)^3}} + m_{12},$$

$$m_{11} = \frac{-a - b + 1 + m}{3ab}, \quad m_{12} = \frac{-a - b + ab}{3ab},$$

$$m_{13} = m_{12}^3 + \frac{(a + b - ab)(m + 1 - a - b) + 3ab}{6a^2b^2}.$$

This study mainly examines the stability variation of the coexisting equilibria point $\overline{E}(u^*, v^*)$ due to introduction of time delay to the model. Acorrding to the equation of u^* and v^*, we have $1 - u^* = \frac{mv^*}{(1+au^*)(1+bv^*)} > 0$, i.e., $1 - u^* > 0$, and it is established that $u^* = v^* \in (0, 1)$.

The linearized system at $\overline{E}\ (u^*, v^*)$ is:

$$\begin{cases} \dfrac{du(t)}{dt} = p\,u(t) + q\,v(t) + d\,u(t-\tau), \\ \dfrac{dv(t)}{dt} = c\,u(t) - c\,v(t), \end{cases}$$

where

$$p = \frac{-3au^{*2} + (2a-2)u^* + 1}{1 + au^*}, \quad q = \frac{u^* - 1}{1 + bv^*} < 0, \quad d = u^* - 1 < 0.$$

The characteristic equation at $\overline{E}\ (u^*, v^*)$ is

$$\begin{vmatrix} \lambda - p - de^{-\lambda\tau} & -q \\ -c & \lambda + c \end{vmatrix} = 0.$$

The eigenvalues λ follows:

$$D(\lambda, \tau) = \lambda^2 + (c - p)\lambda - (p + q)c - (\lambda + c)de^{-\lambda\tau} = 0. \tag{3.1}$$

Ruan and Wei [19] have shown that if every eigenvalue of (3.1) has negative real part, then the equilibrium point is locally asymptotically stable. Next, we will discuss two cases of $\tau = 0$ and $\tau \neq 0$. When $\tau = 0$, Equation (3.1) is reduced to

$$D(\lambda, 0) = \lambda^2 + (c - p - d)\lambda - (p + q + d)c = 0.$$

This is a quadratic equation in λ. If the discriminant is positive, the roots can be obtained using Vieta's theorem. To ensure that both roots possess negative real parts, we impose the following two assumptions:

(H_1) $p < 0$;

(H_2) $(c + p + d)^2 + 4cq > 0$.

Lemma 3.1. *Assuming (H_1) and (H_2), the coexisting equilibrium $\overline{E}(u^*, v^*)$ of model (2.3) should be locally asymptotically stable.*

Thus, the theorem regarding the zero distribution of exponential polynomials in [19] can be applied to analyze the root distribution of Eq (3.1), which is stated as:

Lemma 3.2. *Consider the exponential polynomial*

$$\begin{aligned} P(\lambda, e^{-\lambda\tau_1}, \cdots, e^{-\lambda\tau_m}) = {} & \lambda^n + p_1^{(0)}\lambda^{n-1} + \cdots + p_{n-1}^{(0)}\lambda + p_n^{(0)} \\ & + [p_1^{(1)}\lambda^{n-1} + \cdots + p_{n-1}^{(1)}\lambda + p_n^{(1)}]e^{-\lambda\tau_1} \\ & + \cdots + [p_1^{(m-1)}\lambda^{n-1} + \cdots + p_{n-1}^{(m-1)}\lambda + p_n^{(m-1)}]e^{-\lambda\tau_m} \end{aligned}$$

where, $\tau_i \geq 0 (i = 1, 2, \cdots, m)$ and $p_i^{(j)}$ $(i = 1, \ldots, m-1,\ j = 1, 2, \cdots, n)$ are constants. As $(\tau_1, \tau_2, \cdots, \tau_m)$ vary, the sum of the orders of the zeros of $P(\lambda, e^{-\lambda\tau_1}, \cdots, e^{-\lambda\tau_m})$ on the open right half plane changes only if a zero appears on or crosses the imaginary axis.

For the case of $\tau \neq 0$, let $\lambda = i\omega$ and substitute the value into Eq (3.1). It follows that:

1) $D(0, \tau) = -(p + q + d)c \neq 0$, when $\omega = 0$;

2) $D(i\omega, \tau) = (i\omega)^2 + (c - p)i\omega - (p + q)c - d(i\omega + c)e^{-i\omega\tau} = 0$, when $\omega \neq 0$.

It is straightforward that in the case of (1), $\lambda = 0$ is not the root of Eq (3.1).

Separating the real and imaginary parts yields,

$$-\omega^2 - (p + q)c = d(c\cos\omega\tau + \omega\sin\omega\tau), \tag{3.2}$$

and

$$\omega(c - p) = d(\omega\cos\omega\tau - c\sin\omega\tau). \tag{3.3}$$

Sovling Eqs (3.2) and (3.3), we have

$$\cos\omega\tau = -\frac{p}{d} - \frac{qc^2}{d(c^2 + \omega^2)}, \quad \sin\omega\tau = \frac{-\omega(\omega^2 + qc + c^2)}{d(c^2 + \omega^2)}. \tag{3.4}$$

Then the sum of the squares of the two equations is,

$$\omega^4 + (c^2 + p^2 - d^2 + 2qc)\omega^2 + [(p + q)^2 - d^2]c^2 = 0. \tag{3.5}$$

Let $\omega^2 = \beta$, then Eq (3.5) becomes

$$F(\beta) = \beta^2 + (c^2 + p^2 - d^2 + 2qc)\beta + [(p+q)^2 - d^2]c^2 = 0, \tag{3.6}$$

and the discriminant becomes

$$\triangle = (c^2 + p^2 - d^2 + 2qc)^2 - 4[(p+q)^2 - d^2]c^2. \tag{3.7}$$

Thus, the roots of (3.6) are

$$\beta = \frac{(d^2 - c^2 - p^2 - 2qc) \pm \sqrt{(d^2 - c^2 - p^2 - 2qc)^2 - 4[(p+q)^2 - d^2]c^2}}{2}. \tag{3.8}$$

To analyze the root distribution of Eq (3.6), we give three distinct assumptions:

(H_3) $\triangle > 0, (p+q)^2 - d^2 > 0$, and $c^2 + p^2 - d^2 + 2qc > 0$;

(H_4) $\triangle > 0, (p+q)^2 - d^2 < 0$;

(H_5) $\triangle > 0, (p+q)^2 - d^2 > 0$, and $c^2 + p^2 - d^2 + 2qc < 0$.

It is easy to see that for case of (H_3)–(H_5), Eq (3.6) has no positive roots, one positive root and two positive roots, respectively.

Lemma 3.3. *Under assumptions $(H_1)-(H_3)$, all roots of Eq (3.1) have negative real parts for all $\tau \geq 0$.*

By Hopf bifurcation theorem in [20], we have:

Theorem 3.1. *The coexistence equilibrium $\overline{E}(u^*, v^*)$ of model (2.3) is asymptotically stable for all $\tau > 0$ if assumptions (H_1)–(H_3) hold.*

Suppose the Eq (3.6) has root with positive real part. Without loss of generality, we suppose that it has two positive roots, according to $\omega^2 = \beta$, we have

$$\omega_{\pm} = \frac{\sqrt{2}}{2}\left[(d^2 - c^2 - p^2 - 2qc) \pm \sqrt{(d^2 - c^2 - p^2 - 2qc)^2 - 4[(p+q)^2 - d^2]c^2}\right]^{\frac{1}{2}}. \tag{3.9}$$

Based on Eq (3.4), we solve for τ using the definition of inverse trigonometric functions and obtain the following expression:

$$\tau_j^{\pm} = \frac{1}{\omega_{\pm}}\left[(\pi + \arcsin\frac{\omega_{\pm}^3 + qc\omega_{\pm} + c^2\omega_{\pm}}{d(c^2 + \omega_{\pm}^2)}) + 2\pi j\right] \qquad j = 0, 1, 2 \cdots\cdots$$

Let

$$\tau_0 = min(\tau_0^+, \tau_0^-), \quad \omega_0 = \omega_{\pm}(\tau = \tau_0). \tag{3.10}$$

By the periodicity of the *sine* function, τ can take infinitely many possible values. We choose the smallest positive value of τ near the origin. Namely, when $\tau = \tau_0$, $\pm i\omega_0$ are the pure imaginary roots of Eq (3.1), so we have:

If $(H_1), (H_2)$, and (H_4) hold or $(H_1), (H_2)$, and (H_5) hold, Eq (3.6) has at least one positive root. Hence, Eq (3.1) has at least one pair of purely imaginary roots $\pm i\omega_0$. That is, when $\tau = \tau_0$, all roots of Eq (3.1) except $\pm i\omega_0$ have negative real parts.

If the root of Eq (3.1) $\lambda(\tau) = \alpha(\tau) + i\beta(\tau)$ satisfies $\alpha(\tau_0) = 0$, $\omega(\tau_0) = \omega_0$, we have:

$$\left[\frac{dRe\lambda(\tau_0)}{d\tau}\right]^{-1} = \frac{2\omega_0^4 + (c^2 + p^2 + 2cq - d^2)\omega_0^2 + (c^2 + p^2 + 2cq - d^2)c^2 + 2c^2\omega_0^2}{d^2(c^2 + \omega_0^2)^2}$$

$$= \frac{2\omega_0^2(\omega_0^2 + c^2) + (c^2 + p^2 + 2cq - d^2)(\omega_0^2 + c^2)}{d^2(c^2 + \omega_0^2)^2}$$

$$= \frac{2\omega_0^2 + (c^2 + p^2 + 2cq - d^2)}{d(c^2 + \omega_0^2)} = \frac{F'(\omega_0^2)}{d(c^2 + \omega_0^2)}.$$

If $F'(\omega_0^2) \neq 0$, then the transversality condition $[\frac{dRe\lambda(\tau_0)}{d\tau}]^{-1} \neq 0$ holds. Consequently, we derive the following conclusion concerning the Hopf bifurcation of the model and the stability of the coexisting equilibrium of model (2.3).

Theorem 3.2. *If $F'(\omega_0^2) \neq 0$, then transversality condition $[\frac{dRe\lambda(\tau_0)}{d\tau}]^{-1} \neq 0$ holds; in this case, the coexisting equilibrium $\overline{E}(u^*, v^*)$ is asymptotically stable when $\tau \in [0, \tau_0)$ and unstable when $\tau > \tau_0$. Also, model (2.3) undergoes Hopf bifurcation at $\overline{E}$ when $\tau = \tau_0$ and τ_0 is given by (3.10).*

4. Direction and stability

In Section 3, we established conditions under which model (2.3) experiences a Hopf bifurcation at coexisting equilibrium $\overline{E}$ when $\tau = \tau_0$. In this section, we determine the direction and stability of the periodic solutions that emerge from this bifurcation. To this end, we utilize center manifold theory and the normal form approach as proposed by [20–22].

Let $\bar{u}(t) = u(t) - u^*$, $\bar{v}(t) = v(t) - v^*$, $X_i(t) = x_i(\tau t)$ (i=1,2), $\tau = \tau_0 + \mu$, $\mu \in \mathbb{R}$

$$\begin{cases} \dfrac{du}{dt} = (u + u^*)(1 - u - u^*) - \dfrac{m(u(t-\tau) + u^*)(v + v^*)}{[1 + a(u + u^*)][(1 + b(v + v^*))]}, \\ \dfrac{dv}{dt} = c(v + v^*)(1 - \dfrac{v + v^*}{u + u^*}). \end{cases} \tag{4.1}$$

Normalize the delay $t \longmapsto \frac{t}{\tau}$, then the model (4.1) becomes

$$\begin{cases} \dfrac{du}{dt} = \tau pu + \tau qv + \tau du(t-1) + f_{11}, \\ \dfrac{dv}{dt} = \tau cu - \tau cv + f_{21}, \end{cases} \tag{4.2}$$

where

$$f = \begin{pmatrix} f_{11} \\ f_{21} \end{pmatrix} = \tau \begin{pmatrix} (u + u^*)(1 - u - u^*) - \frac{m(u(t-1)+u^*)(v+v^*)}{[1+a(u+u^*)][1+b(v+v^*)]} - pu - qv - du(t-1) \\ c(v + v^*)(1 - \frac{v+v^*}{u+u^*}) - cu + cv \end{pmatrix}.$$

Model (4.2) is then converted into a funcational differential equation (FDE) in $C = C([-1, 0], \mathbb{R}^2)$, that is,

$$\dot{u}(t) = L_\mu(x_t) + f(\mu, x_t).$$

where, $x(t) = (x_1(t), x_2(t))^T \in \mathbb{R}^2$, $x_t(\theta) = x(t+\theta) \in C$, $L_\mu : C \to \mathbb{R}^2$, and $f : \mathbb{R} \times C \to \mathbb{R}^2$ are given, respectively by

$$L_\mu(\phi) = (\tau_0 + \mu)\begin{pmatrix} p & q \\ c & -c \end{pmatrix}\phi(0) + (\tau_0 + \mu)\begin{pmatrix} d & 0 \\ 0 & 0 \end{pmatrix}\phi(-1), \tag{4.3}$$

$$f(\mu, \phi) = (\tau_0 + \mu)\begin{pmatrix} (\phi_1(0) + u^*)(1 - \phi_1(0) - u^*) - \frac{m(\phi_1(-1)+u^*)(\phi_2(0)+v^*)}{[1+a(\phi_1(0)+u^*)][(1+b(\phi_2(0)+v^*))]} \\ -p\phi_1(0) - q\phi_2(0) - d\phi_1(-1) \\ c(\phi_2(0) + v^*)(1 - \frac{\phi_2(0)+v^*}{-\phi_1(0)+u^*}) - c\phi_1(0) + c\phi_2(0) \end{pmatrix}, \tag{4.4}$$

where $\phi = (\phi_1, \phi_2)^T \in C([-1, 0],\ \mathbb{R}^2)$. $\mu = 0$ is the Hopf-bifurcation point. From the Riesz representation theorem, there must exist a 2×2 matrix $\eta(\theta, \mu)$ $(-1 \le \theta \le 0)$ which has elements of bounded variation functions such that

$$L_\mu(\phi) = \int_{-1}^{0} [d\eta(\theta, \mu)]\phi(\theta), \qquad for\ \phi \in C([-1, 0],\ \mathbb{R}^2). \tag{4.5}$$

When taking

$$\eta(\theta, \mu) = \begin{cases} (\tau_0 + \mu)\begin{pmatrix} p & q \\ c & -c \end{pmatrix}, & \theta = 0, \\ 0, & \theta \in (-1, 0), \\ -(\tau_0 + \mu)\begin{pmatrix} d & 0 \\ 0 & 0 \end{pmatrix}, & \theta = -1. \end{cases} \tag{4.6}$$

Equation (4.5) holds. For $\phi \in C^1([-1, 0],\ \mathbb{R}^2)$, let

$$A(\mu)\phi(\theta) = \begin{cases} \dfrac{d\phi(\theta)}{d\theta}, & \theta \in [-1, 0), \\ \displaystyle\int_{-1}^{0} d\eta(\xi, \mu)\,\phi(\xi), & \theta = 0. \end{cases}$$

and

$$R(\mu)\phi(\theta) = \begin{cases} 0, & \theta \in [-1, 0), \\ f(\mu, \phi), & \theta = 0. \end{cases}$$

Equation (4.5) is rewritten as the following abstract equation:

$$\dot{x}(t) = A(\mu)x_t + R(\mu)x_t, \tag{4.7}$$

where $x = (x_1, x_2)^T$, $x_t = x(t + \theta)$, for $\theta \in [-1, 0]$.

For $\psi \in C^1([0, 1],\ \mathbb{R}^{2^*})$, let

$$A^*\psi(s) = \begin{cases} -\frac{d\psi(s)}{ds}, & s \in (0, 1], \\ \int_{-1}^{0} d\eta^T(t, 0)\psi(-t), & s = 0, \end{cases}$$

and

$$\langle \psi(s)\ ,\ \phi(\theta) \rangle = \bar{\psi}(0)\phi(0) - \int_{-1}^{0}\int_{\xi=0}^{\theta} \bar{\psi}(\xi - \theta)d\eta(\theta)\phi(\xi)d\xi,$$

where $\eta(\theta) = \eta(\theta, 0)$. Then, $A(0)$ and $A^*(0)$ are adjoint operators which share the same eigenvalues, that is, $\pm i\omega_0\tau_0$. Consequently, the eigenvectors of $A(0)$ and $A^*(0)$ must be determined by these eigenvalues.

The vector $q(\theta) = (\frac{i\omega_0+c}{c}, 1)^T e^{i\omega_0\tau_0\theta}$ $(\theta \in [-1, 0])$ is the eigenvector of $A(0)$, i.e., $A(0)q(\theta) = i\omega_0\tau_0 q(\theta)$. Similarly, we can let $q^*(s) = D(1, \frac{i\omega_0+c}{c})e^{i\omega_0\tau_0 s}$ $(s \in [0, 1])$ be the eigenvector of A^* corresponding to $-i\omega_0$. Here, D is constant satisfying $\langle q^*(s), q(\theta)\rangle = 1, \langle q^*(s), \bar{q}(\theta)\rangle = 0$, and $\overline{D} = \frac{c}{2c-(i\omega_0+c)d\tau_0 e^{i\omega_0\tau_0}}$.

Following the notations in [20–22], we compute the coordinates need to describe the center manifold C_0 at $\mu = 0$. Let x_t be the solution of (4.7) when $\mu = 0$, and define

$$z(t) = \langle q^*, x_t\rangle, \quad W(t, \theta) = x_t(\theta) - 2\,\mathrm{Re}\{z(t)q(\theta)\}. \tag{4.8}$$

On the manifold C_0, we obtained:

$$W(t, \theta) = W(z(t), \bar{z}(t), \theta) = W_{20}(\theta)\frac{z^2}{2} + W_{11}(\theta)z\bar{z} + W_{02}(\theta)\frac{\bar{z}^2}{2} + W_3^0(\theta)\frac{z^3}{6} + \cdots,$$

where z and $\bar{z}$ are local coordinates for the manifold C_0 in the directions of q^* and $\bar{q}*$. Meanwhile, W is real if x_t is real. For solution $x_t \in C_0$, since $\mu = 0$, we have

$$\dot{z}(t) = i\omega_0 z(t) + \overline{q^*(0)}f(\mu_0, zq(\theta) + \bar{z}\bar{q}(\theta) + W(z, \bar{z}, \theta)).$$

Let $f_0 = f(\mu_0, zq(\theta) + \bar{z}\bar{q}(\theta) + W(z, \bar{z}, \theta)) = f_{z^2}\frac{z^2}{2} + f_{z\bar{z}}z\bar{z} + f_{\bar{z}^2}\frac{\bar{z}^2}{2} + f_{z^2\bar{z}}\frac{z^2\bar{z}}{2} + \cdots$, then

$$\dot{z}(t) = i\omega_0 z(t) + \overline{q^*(0)}f_0,$$

or

$$\dot{z}(t) = i\omega_0 z(t) + g(z, \bar{z}),$$

where

$$g(z, \bar{z}) = g_{20}\frac{z^2}{2} + g_{11}z\bar{z} + g_{02}\frac{\bar{z}^2}{2} + g_{21}\frac{z^2\bar{z}}{2} + \cdots,$$

and

$$g_{20} = \bar{q}^*(0)f_{z^2}, g_{11} = \bar{q}^*(0)f_{z\bar{z}}, g_{02} = \bar{q}^*(0)f_{\bar{z}^2}, g_{21} = \bar{q}^*(0)f_{z^2\bar{z}}.$$

Following the same algorithms described in [21, 22], we obtain the coefficients by calculation as follows:

$$\begin{aligned}
g_{02} &= \overline{D}\tau_0[h_{12}(\frac{c-i\omega_0}{c})^2 + h_{13}\frac{c-i\omega_0}{c} + 2h_{14} + 2h_{15}(\frac{c-i\omega_0}{c})^2 e^{i\omega_0\tau_0} \\
&\quad +2h_{16}\frac{c-i\omega_0}{c}e^{i\omega_0\tau_0} + \frac{c-i\omega_0}{c}(2h_{23}\frac{c-i\omega_0}{c} + 2h_{22}(\frac{c-i\omega_0}{c})^2 + 2h_{24})], \\
g_{20} &= \overline{D}\tau_0[h_{12}(\frac{c+i\omega_0}{c})^2 + h_{13}\frac{c+i\omega_0}{c} + 2h_{14} + 2h_{15}(\frac{c+i\omega_0}{c})^2 e^{-i\omega_0\tau_0} \\
&\quad +2h_{16}\frac{c+i\omega_0}{c}e^{-i\omega_0\tau_0} + \frac{c-i\omega_0}{c}(h_{23}\frac{c+i\omega_0}{c} + 2h_{22}(\frac{c+i\omega_0}{c})^2 + 2h_{24})], \\
g_{11} &= \overline{D}\tau_0[2h_{12}\frac{c^2+\omega_0^2}{c} + 2h_{13} + 2h_{14} + h_{15}\frac{c^2+\omega_0^2}{c^2}e^{-i\omega_0\tau_0} + h_{15}\frac{c^2+\omega_0^2}{c^2}e^{i\omega_0\tau_0} \\
&\quad +h_{16}\frac{c-i\omega_0}{c}e^{i\omega_0\tau_0} + h_{16}\frac{c+i\omega_0}{c}e^{-i\omega_0\tau_0} + \frac{c-i\omega_0}{c}(ch_{23} + 2h_{22}\frac{c^2+\omega_0^2}{c^2} + 2h_{24})],
\end{aligned}$$

$$
\begin{aligned}
g_{21} &= \overline{D}\tau_0[h_{13}\frac{c+i\omega_0}{c}W_{11}^2(0)+h_{13}\frac{W_{20}^1(0)}{2}+h_{13}W_{11}^1(0)+h_{13}\frac{c+i\omega_0}{c}W_{11}^2(0)\\
&+h_{15}\frac{c+i\omega_0}{c}W_{11}^1(-1)+h_{15}\frac{W_{20}^1(0)}{2}\frac{c-i\omega_0}{c}e^{i\omega_0\tau_0}+h_{15}W_{11}^1(-1)\frac{c+i\omega_0}{c}\\
&+h_{15}W_{11}^1(0)\frac{c+i\omega_0}{c}e^{-i\omega_0\tau_0}+h_{16}(W_{11}^1(-1)+\frac{W_{20}^1(-1)}{2}+\frac{W_{20}^2(0)}{2}\frac{c-i\omega_0}{c}e^{i\omega_0\tau_0}\\
&+W_{11}^2(0)\frac{c+i\omega_0}{c}e^{-i\omega_0\tau_0})+\frac{c-i\omega_0}{c}(h_{23}\frac{c+i\omega_0}{c}W_{11}^2(0)+h_{23}\frac{W_{20}^2(0)}{2}\frac{c-i\omega_0}{c}\\
&+W_{20}^1(0)\frac{c-i\omega_0}{c}+2W_{11}^1(0)\frac{c+i\omega_0}{c}+2W_{11}^2(0)+\frac{1}{2}W_{20}^2(0))],
\end{aligned}
$$

and

$$
\begin{aligned}
h_{12} &= -2-2\frac{amu^*v^*}{(1+au^*)^3(1+bv^*)},\quad h_{13}=\frac{2amu^*}{(1+au^*)^2(1+bv^*)^2},\\
h_{14} &= \frac{2mu^*}{(1+au^*)(1+bv^*)^3},\quad h_{15}=\frac{2amu^*}{(1+au^*)^2(1+bv^*)},\\
h_{16} &= \frac{-2m}{(1+au^*)(1+bv^*)^2},\quad h_{22}=h_{24}=\frac{-2c}{u^*},\quad h_{23}=\frac{4c}{u^*}.
\end{aligned}
$$

We need to calculate $W_{20}(\theta)$ and $W_{11}(\theta)$ appearing in g_{21}. As in [21, 22],

$$
\dot{W}=\dot{x}_t-\dot{z}q-\dot{\bar{z}}\bar{q}=\begin{cases}A(0)W-2\,\mathrm{Re}\{\bar{q}^*(0)f_0q(\theta)\}, & \theta\in[-1,0)\\ A(0)W-2\,\mathrm{Re}\{\bar{q}^*(0)f_0q(\theta)\}+f_0, & \theta=0.\end{cases}\tag{4.9}
$$

Let

$$
H(z,\bar{z},\theta)=\begin{cases}2Re\{\bar{q}^*(0)f_0q(\theta)\}, & \theta\in[-1,0)\\ 2Re\{\bar{q}^*(0)f_0q(\theta)\}+f_0, & \theta=0.\end{cases}
$$

We rewrite (4.9) as

$$
\dot{W}=A(0)W+H(z,\bar{z},\theta)
$$

where

$$
H(z,\bar{z},\theta)=H_{20}(\theta)\frac{z^2}{2}+H_{11}(\theta)z\bar{z}+H_{02}(\theta)\frac{\bar{z}^2}{2}+\cdots.\tag{4.10}
$$

From (4.9), (4.10), and the definition of W, there are

$$
(A(0)-2i\omega_0)W_{20}(\theta)=-H_{20}(\theta),\quad A(0)W_{11}(\theta)=-H_{11}(\theta).\tag{4.11}
$$

From (4.9) and $\theta\in[-1,0)$,

$$
H(z,\bar{z},\theta)=-\bar{q}^*(0)f_0q(\theta)-q^*(0)\bar{f}_0\bar{q}(\theta)=-g(z,\bar{z})q(\theta)-\bar{g}(z,\bar{z})\bar{q}(\theta).
$$

Evaluating coefficients in (4.11),

$$
H_{z^2}=H_{20}(\theta)=-g_{20}q(\theta)-\bar{g}_{02}\bar{q}(\theta),\tag{4.12}
$$

$$
H_{z\bar{z}}=H_{11}(\theta)=-g_{11}q(\theta)-\bar{g}_{11}\bar{q}(\theta).\tag{4.13}
$$

Acorrding to Eqs (4.11)–(4.13) and $A(0)$, we obtain

$$\dot{W}_{20}(\theta) = 2i\omega_0 W_{20}(\theta) + g_{20}q(\theta) + \bar{g}_{02}\bar{q}(\theta),$$

and further,

$$W_{20}(\theta) = \frac{ig_{20}}{\omega_0\tau_0}q(\theta) + \frac{i\bar{g}_{02}}{3\omega_0\tau_0}\bar{q}(\theta) + E_1 e^{2i\omega_0\tau_0\theta}.$$

According to

$$[2i\omega_0\tau_0 I - \int_{-1}^{0} d\eta(\theta)e^{2i\omega_0\theta}]E_1 = h_{z^2},$$

where

$$h_{z^2} = \begin{pmatrix} 2h_{12}(\frac{c+i\omega_0}{c})^2 + h_{13}\frac{c+i\omega_0}{c} + 2h_{14} + 2h_{15}(\frac{c+i\omega_0}{c})^2 e^{-i\omega_0\tau_0} + 2h_{16}\frac{c+i\omega_0}{c}e^{-i\omega_0\tau_0} \\ 2h_{23}\frac{c+i\omega_0}{c} + 2h_{22}(\frac{c+i\omega_0}{c})^2 + 2h_{24} \end{pmatrix},$$

we can obtain $E_1 = (E_1^{(1)},\ E_1^{(2)})^T$, where $E_1^{(i)} = \frac{2\triangle_1^{(i)}}{\triangle_1}$ $(i = 1, 2)$, with

$\triangle_1 = (2i\omega_0 - p + de^{-2i\omega_0\tau_0})(2i\omega_0 + c)\tau_0 - \tau_0 cq,$

$\triangle_1^{(1)} = 2i\omega_0 c(2h_{12}(\frac{c+i\omega_0}{c})^2 + h_{13}\frac{c+i\omega_0}{c} + 2h_{14} + 2h_{15}(\frac{c+i\omega_0}{c})^2 e^{-i\omega_0\tau_0} + 2h_{16}\frac{c+i\omega_0}{c}e^{-i\omega_0\tau_0})$
$+ q(2h_{23}\frac{c+i\omega_0}{c} + 2h_{22}(\frac{c+i\omega_0}{c})^2 + 2h_{24}),$

$\triangle_1^{(2)} = c(2h_{12}(\frac{c+i\omega_0}{c})^2 + h_{13}\frac{c+i\omega_0}{c} + 2h_{14} + 2h_{15}(\frac{c+i\omega_0}{c})^2 e^{-i\omega_0\tau_0} + 2h_{16}\frac{c+i\omega_0}{c}e^{-i\omega_0\tau_0})$
$+ (2i\omega_0 - p + de^{-2i\omega_0\tau_0})(2h_{23}\frac{c+i\omega_0}{c} + 2h_{22}(\frac{c+i\omega_0}{c})^2 + 2h_{24}).$

Similarly, we have

$$\dot{W}_{11}(\theta) = g_{11}q(\theta) + \bar{g}_{11}\bar{q}(\theta),$$

so

$$W_{11}(\theta) = -\frac{ig_{11}}{\omega_0\tau_0}q(\theta) + \frac{i\bar{g}_{11}}{\omega_0\tau_0}\bar{q}(\theta) + E_2.$$

Based on

$$\int_{-1}^{0} d\eta(\theta))E_2 = -h_{z\bar{z}},$$

where

$$h_{z\bar{z}} = 2\begin{pmatrix} h_{12}\frac{c^2+\omega_0^2}{c} + h_{13} + h_{14} + h_{15}\frac{c^2+\omega_0^2}{c^2} + h_{16}(\frac{c-i\omega_0}{c}e^{i\omega_0\tau_0} + \frac{c+i\omega_0}{c}e^{-i\omega_0\tau_0}) \\ ch_{23} + \frac{c^2+\omega_0^2}{c^2} + h_{24} \end{pmatrix},$$

we can obtain $E_2 = (E_2^{(1)},\ E_2^{(2)})^T$, and $E_2^{(i)} = \frac{2\triangle_2^{(i)}}{\triangle_2}$ $(i = 1, 2)$ with

$\triangle_2 = (d - p - q)c\tau_0,$

$\triangle_2^{(1)} = c(h_{12}\frac{c^2+\omega_0^2}{c} + h_{13} + h_{14} + h_{15}\frac{c^2+\omega_0^2}{c^2} + h_{16}(\frac{c-i\omega_0}{c}e^{i\omega_0\tau_0} + \frac{c+i\omega_0}{c}e^{-i\omega_0\tau_0}))$
$+ q(ch_{23} + \frac{c^2+\omega_0^2}{c^2} + h_{24}),$

$\triangle_2^{(2)} = c(h_{12}\frac{c^2+\omega_0^2}{c} + h_{13} + h_{14} + h_{15}\frac{c^2+\omega_0^2}{c^2} + h_{16}(\frac{c-i\omega_0}{c}e^{i\omega_0\tau_0} + \frac{c+i\omega_0}{c}e^{-i\omega_0\tau_0}))$
$+ (d - p)(ch_{23} + \frac{c^2+\omega_0^2}{c^2} + h_{24}).$

Because g_{ij} is explicitly determined by the parameters and delay [20, 22],

$$c_1(0) = \frac{i}{2\omega_0\tau_0}\left(g_{11}g_{20} - 2|g_{11}|^2 - \frac{|g_{02}|^2}{3}\right) + \frac{g_{21}}{2},$$

$$\mu_2 = -\frac{Re(c_1(0))}{Re(\lambda'(\tau_0))},$$

$$T_2 = -\frac{Imc_1(0) + \mu_2 Im\lambda'(\tau_0)}{\omega_0\tau_0},$$

$$\beta_2 = 2Re(c_1(0)).$$

Theorem 4.1. *We choose τ_0, then we have*

1) the sign of μ_2 indicates whether Hopf bifurcation can occur either forward ($\mu_2 > 0$) or backward ($\mu_2 < 0$);

2) $\beta_2 < 0$ ($\beta_2 > 0$) means the bifurcate periodic solutions on the center manifold are stable (unstable);

3) $T_2 > 0$ ($T_2 < 0$) implies the period increases (decreases).

5. Numerical simulations and discussion

To verify the theoretical results obtained in the previous sections, we perform numerical simulations. The parameters are chosen according to the conditions derived from stability and bifurcation analyses. Specifically, we consider two sets of parameters to capture different dynamical regimes: (i) parameters satisfying the stability condition to demonstrate the asymptotic stability of the equilibrium; (ii) parameters crossing the Hopf bifurcation threshold to illustrate the emergence of periodic solutions. The parameters are selected from existing literature to ensure ecological interpretability. Through these simulations, we aim to visualize the effects of key factors on the dynamical behavior of the predator-prey model.

The parameters are selected as:

1) $m = 0.83, a = 0.52, b = 0.12, c = 0.92$.

This parameter set fulfills all conditions required in Theorem 3.1. The coexistence of equilibrium $\overline{E}(0.63273, 0.63273)$ with initial functional $\phi(\theta) = (0.73, 0.71), \theta \in (-\tau, 0]$ is asymptotically stable for all values of $\tau > 0$. The corresponding population oscillation situation is as shown in Figure 1 when $\tau = 5.8096$. For $\tau = 30.8096$, we observe that the densities of the two populations fluctuate over a long time and eventually converge to the equilibrium (Figure 2).

Despite a substantial increase in time delay relative to Figure 1, the system remains stable. Both the prey population $u(t)$ and predator population $v(t)$ converge to the equilibrium point as time evolves. This indicates that within this parameter regime, the coexisting equilibrium maintains its asymptotic stability even for large time delays. Such stability at large delays, together with the instability arising at intermediate delay values, verifies the existence of multiple stability switches, consistent with the predictions of our theoretical analysis.

We select an alternative set of settings that satisfies Theorem 3.2:

2) $m = 0.863, a = 0.172, b = 0.362, c = 0.1$.

From (3.10), $\tau_0 = 5.1689$, $\omega_0 = 0.1965$, and $c_1(0) = -2.38747 + i0.16027$. From Theorem 3.2, the equilibrium $\overline{E}(0.611724, 0.611724)$ of the delay model (2.3) with initial functional (0.73, 0.71) is asymptotically stable when $\tau = 5.1034 < \tau_0$ (Figure 3). There is a Hopf bifurcation at $\tau = \tau_0$, and the periodic solution arising from this bifurcation is orbitally asymptotically stable for $\tau = 5.9676$, which is greater than τ_0 (Figure 4).

The oscillation amplitude increases as the delay rises, suggesting that longer predator handling times result in more pronounced population fluctuations. Both orbits are orbitally asymptotically stable, and trajectories starting near either orbit converge to the corresponding limit cycle.

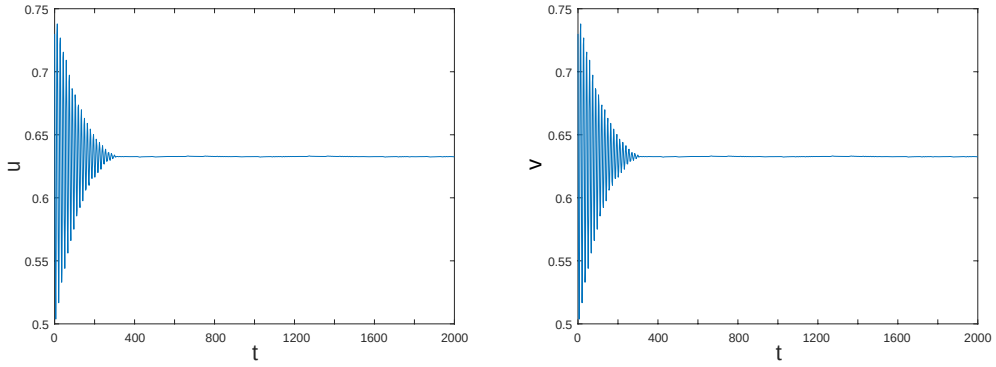

Figure 1. For the delay $\tau = 5.8096 > 0$ and initial function $\phi(\theta) = (0.73, 0.71)$ with $\theta \in (-\tau, 0]$, both populations converge to the coexisting equilibrium $\overline{E}(0.63273, 0.63273)$, which demonstrates its asymptotic stability.

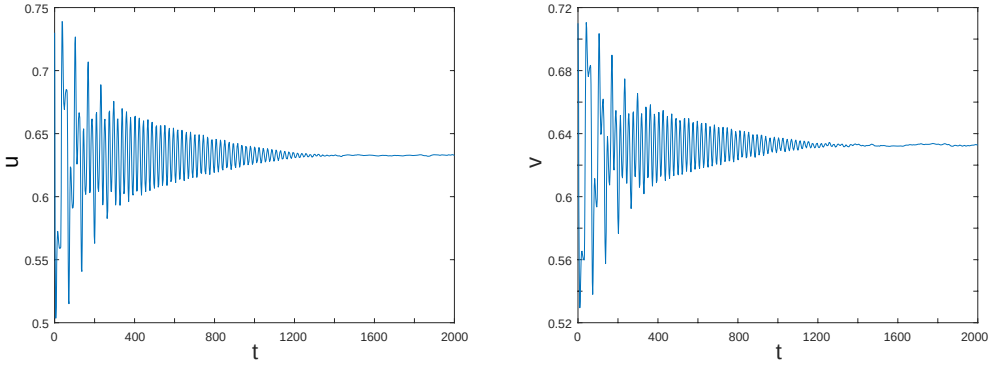

Figure 2. For the delay $\tau = 30.8096 > 0$ and initial function $\phi(\theta) = (0.73, 0.71)$ with $\theta \in (-\tau, 0]$, both populations converge to the coexisting equilibrium $\overline{E}(0.63273, 0.63273)$, which demonstrates its asymptotic stability despite the large delay value.

Model (2.1) exhibits Hopf bifurcation, stability switches, and double Hopf bifurcation, leading to complex periodic or quasi-periodic behaviors. Such complexity originates from the infinitely many critical values $\tau_j^{\pm}$. There exists a positive integer k such that the stability $\overline{E}$ swithes back and forth k times if (H_1), (H_2), and (H_5) are met, ultimately resulting in occurrence of double Hopf bifurcation. The figures illustrate the dynamical evolution as τ increases: for small τ, the system merges to a steady state; when τ exceeds τ_0, a stable period-1 solution emerges via Hopf bifurcation; as τ increases further, the period-1 solution loses stability, giving rise to solutions with periods-2, periods-4, and periods-8 solutions (Figure 5), which may eventually evolve into a chaotic attractor. A theoretical interpretation of these phenomena via the center manifold theorem and normal form theory remains to be further investigated.

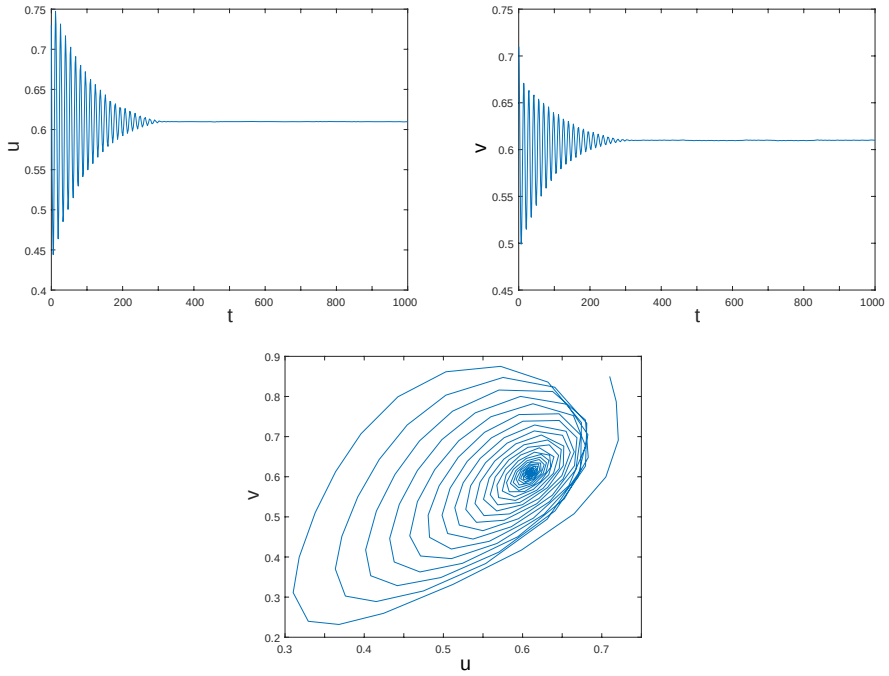

Figure 3. The coexisting equilibrium $\overline{E}(0.611724, 0.611724)$ is asymptotic stability for $\tau = 5.1034 < \tau_0 = 5.1689$. Under initial functional (0.73, 0.71), both populations converge to the equilibrium, consistent with the theoretical stability criterion.

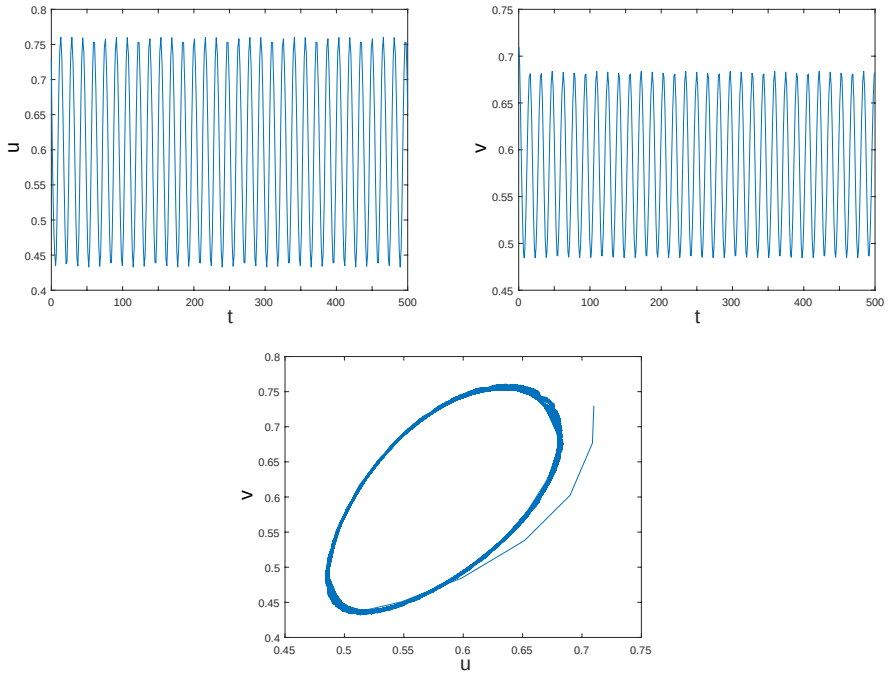

Figure 4. With the delay $\tau = 5.9676 > \tau_0 = 5.1689$, the coexisting equilibrium loses stability, and a stable limit cycle emerges.

Numerical simulations confirm that the Hopf bifurcation is supercritical. Once the critical threshold is crossed, the system no longer converges to the equilibrium but exhibits sustained oscillations, indicating the emergence of a stable bifurcating periodic solution.

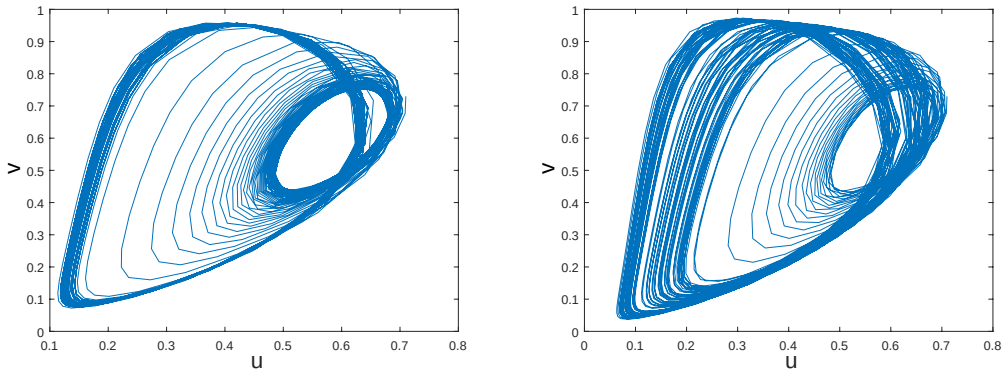

Figure 5. Stable periodic orbits (limit cycles) of model (2.3) for two delay values τ=5.9686 and τ=6.1076. Both delays exceed the Hopf bifurcation threshold τ_0=5.1689.

6. Conclusions

In this paper, we perform rigorous mathematical analysis and numerical simulations to explore the dynamical characteristics of a delayed predator-prey model with the Crowley-Martin functional response. We derive the stability criteria for the coexisting equilibrium and prove that time delays can induce Hopf bifurcation and destabilize the model. The bifurcating periodic solutions are investigated for their stability, and the bifurcation direction is determined. Through numerical simulations using MATLAB, we have extended the local bifurcation analysis to a global perspective. The results show that stable periodic solutions exist for wide delay ranges. Moreover, as the time delay lengthens, the coexisting equilibrium alternates between stability and instability multiple times, leading to the occurrence of double Hopf bifurcations. These findings reveal the complex dynamical behavior arising from the interplay between the Crowley-Martin functional response and time delay, offering a deeper understanding of the oscillatory dynamics in predator-prey frameworks.

From a biological perspective, these results suggest that when the predator's handling time exceeds a critical threshold, the response delay can drive sustained population cycles. However, a further increase in the delay may sometimes restore stability-which constitutes a counterintuitive phenomenon and provides crucial implications for understanding oscillatory dynamics in real ecosystems. At the application level, our results identify specific delay thresholds that can be estimated from field data, providing a basis for biological control and wildlife management strategies.

Use of AI tools declaration

The authors declare they have not used Artificial Intelligence (AI) tools in the creation of this article.

Acknowledgments

The Heilongjiang Provincial Natural Science Foundation of Funder provided funding (No. LH2022A001) for this work, and by the the Daqing Normal University Natural Science Foundation Of Funder (No. 19ZR01).

Conflicts of interest

The authors declare there is no conflict of interest.

References

1. P. A. Abrams, The evolution of predator-prey interactions: Theory and evidence, *Annu. Rev. Ecol. Evol. Syst.*, **31** (2000), 79–105. https://doi.org/ 10.1146/annurev.ecolsys.31.1.79
2. M. Chen, Y. Takeuchi, J. Zhang, Dynamic complexity of a modified Leslie-Gower predator-prey system with fear effect, *Commun. Nonlinear Sci. Numer. Simul.*, **119** (2023), 107109. https://doi.org/10.1016/j.cnsns.2023.107109
3. S. Guo, W. Jiang, Hopf-fold bifurcation and fluctuation phenomena in a delayed ratio-dependent Gause-Type predator-prey model, *Int. J. Bifurcation Chaos*, **23** (2013), 1350153. https://doi.org/10.1142/s0218127413501538
4. M. Yang, Y. Nie, Bifurcation analysis of a delayed predator-prey model with Holling-III functional response, *Z. Angew. Math. Phys.*, **75** (2024), 240. https://doi.org/10.1007/s00033-024-02376-8
5. X. Chen, Y. Qi, M. Wang, A strongly coupled predator-prey system with non-monotonic functional response, *Nonlinear Anal. Theory Methods Appl.*, **67** (2007), 1966–1979. https://doi.org/10.1016/j.na.2006.08.022
6. H. Baek, A food chain system with Holling type IV functional response and impulsive perturbations, *Comput Math Appl.*, **60** (2010), 1152–1163. https://doi.org/10.1016/j.camwa.2010.05.039
7. Y. Qiao, H. Cao, G. Xu, A double time-delay Holling II predation model with weak Allee effect and age-structure, *Electron. Res. Arch.*, **32** (2024), 1749–1769. https://doi.org/10.3934/era.2024080
8. L. Wang, R. Xu, G. Feng, A stage-structured predator-prey system with time delay, *J. Appl. Math. Comput.*, **33** (2010), 267–281. https://doi.org/10.1007/s12190-009-0286-x
9. H. Shi, S. Ruan, Spatial, temporal and spatiotemporal patterns of diffusive predator-prey models with mutual interference, *IMA J. Appl. Math.*, **80** (2015), 1534–1568. https://doi.org/10.1093/imamat/hxv006
10. P. H. Crowley, E. K. Martin, Functional response and interference within and between year classes of a dragonfly population, *J. North Am. Benthological Soc.*, **8** (1989), 211–221. https://doi.org/10.2307/1467324
11. A. P. Maiti, B. Dubey, J. Tushar, A delayed prey-predator model with Crowley-Martin-type functional response including prey refuge, *Math. Methods Appl. Sci.*, **40** (2017), 5792–5809. https://doi.org/10.1002/mma.4429

12. D. Wang, Y. Ma, Bifurcation and turing pattern formation in a diffusion modified Leslie-Gower predator-prey model with Crowley-Martin functional response, *J. Appl. Math. Phys.*, **12** (2024), 2190–2211. https://doi.org/10.4236/jamp.2024.126133
13. Y. Guo, S. Sun, Dynamic behavior of a stochastic non-autonomous predator-prey model with Crowley-Martin functional response and impulses, *J. Biol. Syst.*, **30** (2022), 183–223. https://doi.org/10.1142/S0218339022500061
14. U. Kumar, A. Kanaujiya, Global dynamics of a prey-predator model with component allee effect for predator reproduction and Crowley-Martin-type functional response:the role of strong Allee effect, *Eur. Phys. J. Plus*, **139** (2024), 878. https://doi.org/10.1140/epjp/s13360-024-05628-8
15. M. Yuan, N. Wang, Stability and bifurcation analysis for a predator-prey model with Crowley-Martin functional response, *J. Nonlinear Model. Anal.*, **7** (2025), 1–19. https://doi.org/10.12150/jnma.2025.1
16. H. Wang, S. Liu, H. Li, Prey-taxis as a driver of spatial patterns in predator-prey systems: From spots to spirals and chaos, *Chaos*, **36** (2026), 013114. https://doi.org/10.1063/5.0312345
17. M. Liu, H. Wang, W. Jiang, Bifurcations and pattern formation in a predator-prey model with memory-based diffusion, *J. Differ. Equations*, **350** (2023), 1–40. https://doi.org/10.1016/j.jde.2022.12.010
18. M. Wang, N. Liu, Qualitative analysis and traveling wave solutions of a predator-prey model with time delay and stage structure, *Electron. Res. Arch.*, **32** (2024), 2665–2698. https://doi.org/10.3934/era.2024121
19. S. Ruan, J. Wei, On the zeros of a third degree exponential polynomial with applications to a delayed model for the control of testosterone secretion, *IMA J. Math. Appl. Med. Biol.*, **18** (2001), 41–52. https://doi.org/10.1093/imammb/18.1.41
20. J. K. Hale, *Theory of Functional Differential Equations*, 2^{nd} edition, Springer, 1977. https://doi.org/10.1007/978-1-4612-9892-2
21. Z. Wei, B. Zhu, J. Yang, M. Perc, M. Slavinec, Bifurcation analysis of two disc dynamos with viscous friction and multiple time delays, *Appl. Math. Comput.*, **347** (2019), 265–281. https://doi.org/10.1016/j.amc.2018.10.090
22. T. Faria, L. T. Magalhaes, Normal forms for retarded functional differential equations with parameters and applications to Hopf bifurcation, *J. Differ. Equations*, **122** (1995), 181–200. https://doi.org/10.1006/jdeq.1995.1144

AIMS Press